Analytica Chimica Acta 981 (2017) 41–52

Contents lists available at ScienceDirect

Analytica Chimica Acta

journal homepage: www.elsevier.com/locate/aca

Electrochemical detection of cardiac biomarker myoglobin using polyphenol as imprinted polymer receptor

J.A. Ribeiro [a, b, **], C.M. Pereira [a, *], A.F. Silva [a], M. Goreti F. Sales [b]

[a] CIQUP/Department of Chemistry and Biochemistry, Faculty of Sciences, University of Porto, Portugal
[b] BioMark/CINTESIS-ISEP, School of Engineering, Polytechnic Institute of Porto, Portugal

HIGHLIGHTS

- Electrochemical biosensor for the detection of an important cardiac biomarker, the hemeprotein Myoglobin.
- MIPs and Screen-Printed Electrode were combined for the simple and fast screening of myoglobin in point-of-care.
- Synthetic receptor prepared by electropolymerization of phenol on Au in the presence of myoglobin as template molecule.
- Determination of serum myoglobin levels with unprecedented sensitivity (detection limit of few pg/mL).

GRAPHICAL ABSTRACT

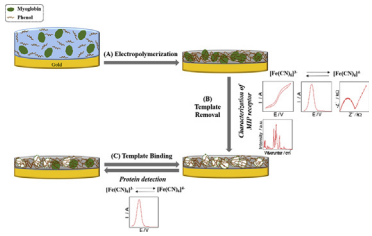

ARTICLE INFO

Article history:
Received 7 March 2017
Received in revised form
5 May 2017
Accepted 12 May 2017
Available online 2 June 2017

Keywords:
Biosensor
Myoglobin
Polyphenol
Molecular imprinting
Screen-printed gold electrode
Synthetic receptor

ABSTRACT

An electrochemical biosensor was developed by merging the features of Molecular Imprinting technique and Screen-Printed Electrode (SPE) for the simple and fast screening of cardiac biomarker myoglobin (Myo) in point-of-care (POC).

The MIP artificial receptor for Myo was prepared by electrooxidative polymerization of phenol (Ph) on a AuSPE in the presence of Myo as template molecule. The choice of the most effective protein extraction procedure from the various extraction methods tested (mildly acidic/basic solutions, pure/mixed organic solvents, solutions containing surfactants and enzymatic digestion methods), and the optimization of the thickness of the polymer film was carefully undertaken in order to improve binding characteristics of Myo to the imprinted polymer receptor and increase the sensitivity of the MIP biosensor. The film thickness was optimized by adjusting scan rate and the number of cycles during cyclic voltammetric electropolymerization of Ph. The thickness of the polyphenol nanocoating of only few nanometres (~4.4 nm), and similar to the protein diameter, brought in significant improvements in terms of sensor sensitivity.

The binding affinity of MIP receptor film was estimated by fitting the experimental data to Freundlich isotherm and a ~8 fold increase in the binding affinity of Myo to the imprinted polymer ($K_F = 0.119 \pm 0.002$ ng^{-1} mL) when compared to the non-imprinted polymer ($K_F = 0.015 \pm 0.002$ ng^{-1} mL) which demonstrated excellent (re)binding affinity for the imprinted protein.

* Corresponding author.
** Corresponding author. CIQUP/Department of Chemistry and Biochemistry, Faculty of Sciences, University of Porto, Portugal.
E-mail addresses: jadribeiro@gmail.com (J.A. Ribeiro), cmpereir@fc.up.pt (C.M. Pereira).

http://dx.doi.org/10.1016/j.aca.2017.05.017

The incubation of the Myo MIP receptor modified electrode with increasing concentration of protein (from 0.001 ng mL^{-1} to 100 μg mL^{-1}) resulted in a decrease of the ferro/ferricyanide redox current. LODs of 2.1 and 14 pg mL^{-1} were obtained from calibration curves built in neutral buffer and diluted artificial serum, respectively, using SWV technique, enabling the detection of the protein biomarker at clinically relevant levels.

The prepared MIP biosensor was applied to the determination of Myo spiked serum samples with satisfactory results.

1. Introduction

Cardiovascular disease (CVD) is one of the world's leading cause of human morbidity and mortality in both developing and developed countries. The early and quick diagnosis of cardiovascular disease is extremely important and crucial not for only patient survival but also saving cost and great deal of time in successful prognosis of the diseases. Therefore, the accurate simultaneous quantification of the most prominently used cardiac markers, such as C-reactive protein (CRP), cardiac troponins, Creatine kinase MB subform (CK-MB) and Myoglobin (Myo), among others, is critical in assisting the quick diagnosis of CVD [1–3].

Myo is a ~18 kDa oxygen-carrying monomeric hemeprotein found in heart and skeletal muscles whose primary function is the uptake of oxygen from oxy-hemoglobin in the bloodstream [4,5]. Besides her biological importance, Myo has also the particularity of being is the first marker released into the circulation after acute myocardial injury (early as 1 h upon symptom) [1–3]. Thus, the determination of serum Myo levels can be a powerful tool in clinical and diagnosis field as key biomarker of cardiac injury at the very first period of disease onset. The clinically significant sensing ranges (cut off levels) of Myo are comprised between 70 and 200 ng mL^{-1} [1] and therefore, assay methods for this biomarker need to be highly sensitive.

Most of the methods reported for detecting Myo rely on immunoassays with different signal transduction, such as fluorescence based micromosaic immunoassay [6], SPR sensor [7], fiber-optic biosensor [8], colorimetric determination with PDMS-AuNPs composite film [9], chemiluminometric ELISA biosensor [10] and electrochemical immunosensors [11–13].

Although some of the methodologies are very accurate and highly selective towards the cardiac biomarker, these methodologies are based on natural receptors (antibodies, enzymes, nucleic acids) as biorecognition element and the preparation of these sensors can be time-consuming, technically complicated (as antibody activity is not easy to maintain in presence of external redox mediators or outside of the physiological environments/synthetic buffers) and rather expensive [14]. Furthermore, the development of novel biorecognition elements that can replace classical antibodies is currently a topic of interest in biosensor technology, aiming to overcome some of the disadvantages related to immunosensors.

In recent years, growing interest in molecularly imprinted polymers (MIPs) in the preparation of recognition elements has led researchers to design novel formats for electrochemical sensors [15,16]. Molecular imprinting is a versatile technique providing synthetic functional materials able to recognize and in some cases respond to biological and chemical agents of interest, such as proteins [17–19], replacing (or complementing) natural receptors. Once polymerization is complete, the template molecule can be extracted with a suitable approach in order to allow the specific recognition sites created by the imprinting process to be available for binding. A flexible MIP may mimic the biological antibody model, although the nature of the polymer may lead to robustness and longevity inherent in a rigid polymer [14,20].

Molecular imprinting based on the electrochemical approach has been considered to be an appealing strategy for development of advanced sensors for protein detection. In comparison to other procedures of MIP film preparation, such as drop-coating, composite making and spin-coating, the MIP films prepared by electropolymerization have superior properties with respect to adherence to the transducer surface as well as simplicity and speed of preparation. Moreover, the electropolymerization enables easy control of the film thickness and morphology as well as high reproducibility and the possibility of polymer preparation and operation in aqueous solutions. Electropolymerization can be performed under galvanostatic, potentiostatic, or most commonly potentiodynamic conditions [15,16].

Phenol (Ph) is well known for its ability to foul electrodes and the tarry deposit formed on electrodes during Ph oxidation is attributed to polymerization products. However, new insights were introduced after deliberate electropolymerization of polyphenols used for entrapping of redox enzymes at electrode surfaces during the preparation of amperometric biosensors [21]. After this first approach, Ph based MIP films used as recognition units in sensors emerged in literature because of their straightforward preparation and ability of these films to interact with many different analytes through π–π stacking.

One of the first successful examples of electrosynthesised polyphenol MIPs was for imprinting phenylalanine [22], leading to the development of the first capacitive sensor possessing a receptor layer consisting of an MIP. MIP polyphenol films were also used in the fabrication of sensing devices for the antibiotic rifamycin SV (RSV) [23], theophylline [24] and methyl viologen [25]. A polyphenol-functionalized imprinted boronic acid served for enantioselective chronoamperometric determination of monosaccharides [26]. In recent pioneer work, a protein-templated MIP Ph film was potentiodynamically deposited on the tips of arrayed carbon nanotubes to fabricate an ultrasensitive impedimetric chemosensor for human ferritin and E7 oncoprotein derived from human papillomavirus [27]. Molecular imprinting methodology was also reported in the literature for the electrochemical detection of Myo [28–32], although these biosensors were not able to detect Myo at physiological levels of interest (cut-off values range from 70 to 200 ng mL^{-1} [1]); these works were capable of detecting only from 0.13 to 8 μg/mL as the minimum limit of detection achieved.

In this work, the great features of molecularly imprinting technique based on electropolymerization, such as good mechanical and chemical stability, ease of preparation, and the relatively low cost of MIP materials were combined with the advantages of screen-printed electrodes (SPEs), namely being simple, inexpensive and versatile to use, to develop a miniaturized point-of-care biosensor for Myo detection with high sensitivity and selectivity. The design and synthesis of the synthetic receptor units for Myo

was based on the electropolymerization of polyphenol in the presence of Myo as template molecule on AuSPE (see Scheme 1). After the extraction of the protein from the matrix the specific binding sites are available for the rebinding of the protein. The experimental conditions affecting the electrochemical detection of the protein, such as the MIP film thickness and the effective extraction of the protein template from the polymeric matrix, were carefully optimized in this work aiming to increase the analytical response of the biosensor to the protein.

2. Experimental

2.1. Chemicals and solutions

Myoglobin (Myo, from equine heart, ≥ 90%, Sigma), phenol (Ph, pure, Panreac), potassium ferricyanide ($K_3[Fe(CN)_6]$, ≥ 99.0%, Fluka), and potassium ferrocyanide ($K_4[Fe(CN)_6].3H_2O$, p.a., ≥ 99.5%, Fluka) were used as received. Phosphate buffer solution (PBS) 0.1 M pH 7.0 consisted of sodium dihydrogen phosphate dihydrate (p.a., Sigma-Aldrich) and anhydrous disodium hydrogen phosphate (p.a., Fluka). Standard stock solution of Myo 1.0 mg mL^{-1} was prepared in PBS 0.1 M at pH 7.0 and stored at −20 °C if not in use. Less concentrated standards were obtained by accurate dilution of the previous solution, in the same buffer. $K_3[Fe(CN)_6]$)/$K_4[Fe(CN)_6]$ (1:1, 5 mM) redox probe solution was prepared in 0.1 M Na_2SO_4. Unless otherwise stated, all the other chemicals and reagents used are of analytical grade. All aqueous solutions were prepared using water purified with a Milli-RO3 Plus and Milli-Q purification systems (resistivity ≥ 18 MΩ cm^{-2}).

2.2. Apparatus

Electrochemical data were obtained using a computer-controlled potentiostat Autolab PGSTAT10 (Eco Chemie B.V., Utrecht, Netherlands) monitored by the NOVA 1.11 software package.

Gold screen-printed electrodes (AuSPEs) were purchased from DropSens (DRP-220AT). They include a gold disk-shaped (12.6 mm^2) working electrode, a silver pseudo-reference electrode and a gold counter electrode, all of them screen-printed on a ceramic substrate (3.3 cm × 1.0 cm) and subjected to high-temperature curing. All potential values were referred to the screen-printed silver pseudo-reference electrode. The SPEs were connected to a switch box, also from DropSens (DRP-DSC), allowing their interface with the potentiostat. All experiments were carried out at room temperature (25 °C).

Raman spectrometry with confocal microscopy measurements were performed using a Thermo Scientific DXR Raman microscope equipped with a 532 nm laser, in combination with a 50 × objective magnification for focusing and collection of Raman-scattered light. An incident maximum laser power of 1 mW was applied in order to avoid peak shifts due to thermal heating or structure transformations during data acquisition. Raman spectra were collected with a slit aperture of 25 μm.

2.3. Preparation of MIP receptor

Prior to modification, the AuSPEs were washed thoroughly with ethanol and acetone followed by electrochemical cleaning by cycling the electrode potential from 0 to 1.1 V at a rate of 100 mV s^{-1} in 0.1 M sulfuric acid until the CV becomes stable (approximately 12 cycles). Finally, the electrodes were washed with ultrapure water.

Although the electrochemical oxidation of Ph can be performed in acidic [33] and alkaline [34] medium, in this work Ph electropolymerization was conducted at neutral pH which is more suitable when working with proteins. Myo-imprinted polyphenol films were deposited on AuSPEs by electropolymerizing 10 mM Ph in PBS 0.1 M at pH 7.0 in the presence of 5 mg mL^{-1} of Myo.

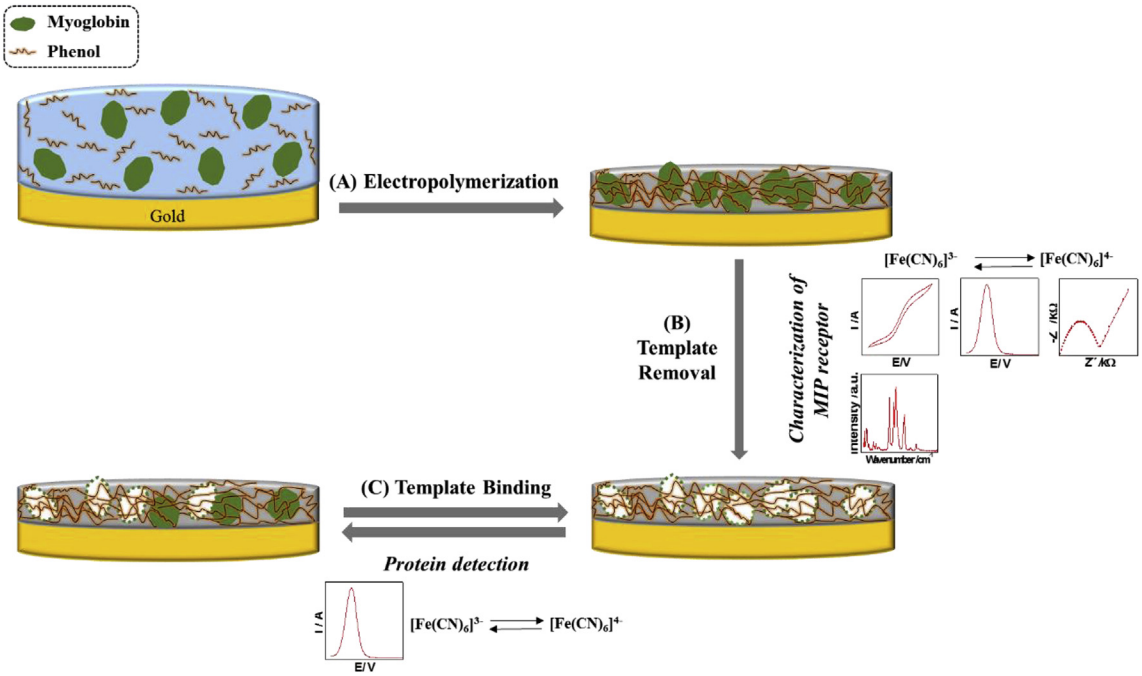

Scheme 1. Schematic representation of molecular imprinting and the recognition principle of the MIP sensor for Myo detection: (A) Template and functional monomer interact to form the binding sites preserved by electropolymerization of Ph; (B) Removal of the template leaves rebinding cavities. Electrochemical (CV, SWV and EIS in the presence of $[Fe(CN)_6]^{3-/4-}$ redox probe) and Raman spectroscopy characterization of MIP electrode was performed at this point; (C) Template rebinding at binding sites, which allows the electrochemical detection of the protein by the prepared MIP electrode, using SWV (in the presence of $[Fe(CN)_6]^{3-/4-}$ redox probe).

Electropolymerization was carried by collecting 1 cyclic voltammogram between −0.3 and 0.8 V at the scan rate of 100 mV s^{-1}. A similar procedure, excluding the presence of Myo, was employed in the fabrication of control non-imprinted polymer (NIP) modified electrodes. The resulting modified electrodes were thoroughly rinsed with pure water to wash away remains of the reactants, dried under a nitrogen flow and stored properly at room temperature for further use.

Different strategies were applied in this work for the effective extraction of Myo from the imprinted surfaces. Myo was successfully washed out from the polymeric matrix after the treatment of MIP surfaces with 20 mM sodium dodecyl sulphate (SDS, ≥ 99.0%, Merck) dissolved in a mixture of PBS 0.1 M pH 7.0/methanol (10:1, v/v) overnight, followed by subsequent extensive washing with ultrapure water.

For characterization of the polymerized films before and after template removal several electrochemical techniques (CV, SWV and EIS) in the presence of ferro/ferricyanide redox probe were utilized. Each of the following post-polymerization treatments were also performed on NIP electrodes as a control, to confirm the success of the extraction procedure tested without destroying the backbone of the polymer network.

2.4. Electrochemical measurements

In order to characterize the imprinted electrodes, electrochemical measurements were carried out in the presence of 5 mM $K_3[Fe(CN)_6]/K_4[Fe(CN)_6]$ (1:1) solution containing 0.1 M Na_2SO_4. The modified surfaces were coated with a 45 μL drop of the redox probe solution.

The careful choice of supporting electrolyte used is of great important in order to increase the sensitivity of the analytical methodology. The electrochemical response of 5 mM $Fe(CN)_6^{4-}$/$Fe(CN)_6^{3-}$ redox pair at bare AuSPE under different background electrolytes was evaluated (see Fig. S1). The electrode produced a well-defined redox peak and higher peaks currents with 0.1 M Na_2SO_4 when comparing to PBS (0.01 and 0.1 M).

Cyclic voltammetry (CV) was performed at a scan rate of 50 mV s^{-1} and square wave voltammetry (SWV) operated under the following conditions: step potential = 2 mV, pulse amplitude = 50 mV and frequency = 25 Hz. Voltammograms collected with the imprinted electrode were recorded in the potential range of −0.1–0.35 V. The potential window over which the electrode performs was carefully chosen in order to avoid the formation of Prussian blue at the AuSPE surface (around 0.5 V; data not shown) due to the reaction of polyphenol with ferricyanide ion [35].

Electrochemical Impedance Spectroscopy (EIS) measurements were performed using a frequency scan ranging from 10,000 to 0.01 Hz and a sine wave perturbation of 10 mV rms. 60 frequency values were collected at the formal potential of the $[Fe(CN)_6]^{3-/4-}$ redox couple. Experimental spectra were presented in the form of complex plane diagrams (i.e., Nyquist plots) and were fitted with proper equivalent circuits using the facilities of the NOVA 1.11 software.

Binding isotherm was fitted to experimental data by non-linear least squares regression analysis using Igor Pro 6.22A software.

2.5. Calibration curves and binding affinity of Myo MIP receptor

The sensor response to Myo was monitored by the development of the corresponding calibration curves. The procedure consisted of incubating the synthetic receptor electrode for 10 min with the appropriate concentration of Myo (from 0.001 ng mL^{-1} to 100 μg mL^{-1}, in 0.1 M PBS pH 7.0) followed by washing with water to remove any loosely bound materials that could have been absorbed at the surface. This solution was then replaced by a drop of the 5 mM $[Fe(CN)_6]^{3-/4-}$ redox probe solution for the electrochemical measurements. Calibration curves were obtained by SWV measurements. A control monitoring was also performed with NIP receptor film.

The concentration of the redox probe solution was optimized in order to increase the electroanalytical signal obtained. Calibration curves for Myo were built using 1, 5 and 10 mM redox probe solutions and the highest sensitivity was obtained with the concentration of 5 mM (data not shown). Also, no improvement was observed in the performance of the MIP sensor by increasing the protein incubation time at the electrode surface from 10 to 30 min. Thus, t_{inc} = 10 min was used, decreasing considerably the time of analyses (data not shown).

To demonstrate the feasibility of the MIP biosensor in practical analysis, artificial serum samples containing known concentrations of Myo were analysed. The artificial serum solution contained [36]: 4.5 mM KCl (Fluka), 5.0 mM $CaCl_2$ (≥97.0%, Fluka), 1.6 mM $MgCl_2$ (p.a., Riedel-de Haen), 4.7 mM D(+)-glucose (Merck), 2.5 mM urea (puriss, Sigma-Aldrich), 0.1% bovine serum albumin (BSA, ≥ 96%, Sigma) and 145 mM NaCl (suprapur, Merck).

Myo samples and standard solutions were prepared by dilution of serum 10 times in PBS 0.1 M pH 7.0. Myo determination in synthetic serum samples was also performed by SWV measurements.

3. Results and discussion

The concept of MIP biosensor is based on the modification of a transducer surface by arranging monomers around a target analyte to provide the formation of specific imprints in polymers and the subsequent template removal from the polymer formed, showing high specificity to the analyte. The binding of the target protein is measured electrochemically by following of the redox behaviour of a probe reaction at the modified electrode.

In this work, a MIP receptor was prepared by electrochemical polymerization of Ph on a AuSPE in the presence of Myo as template molecule and optimum conditions for template removal were established (see Scheme 1). The surface characteristics, such as the film thickness, concentration of monomer/template used, etc., were carefully optimized in order to increase the analytical performance of the MIP biosensor for Myo determination in both buffer and serum.

3.1. Thickness of polyphenol film

During the imprinting process, the formation of an ultrathin polymer film on the transducer surface was preferred to improve the sensitivity of the device. For this purpose, the thickness of polyphenol film was adjusted by controlling the scan rate and the number of cycles during cyclic voltammetric electropolymerization on AuSPE.

Preliminary experiments conducted on NIP surfaces were performed in order to study the effect of scan rate during electropolymerization of polyphenol. The voltammograms recorded during 1 cycle electrodeposition of Ph on bare AuSPEs at different scan rate are shown in Fig. 1A. The mechanism associated with the oxidation of Ph on metal electrodes involves the reaction of the electrogenerated phenoxy radical (observed at ~0.6 V) with a further Ph molecule to yield a predominantly *para*-linked dimeric radical; subsequent reactions produce a neutral dimer, oligomers and finally a passivating ultrathin insulating film [33,34,37].

The CVs collected at the electropolymerized NIP receptor, shown in Fig. 1B, indicates the deposition of a non-conducting polymer at

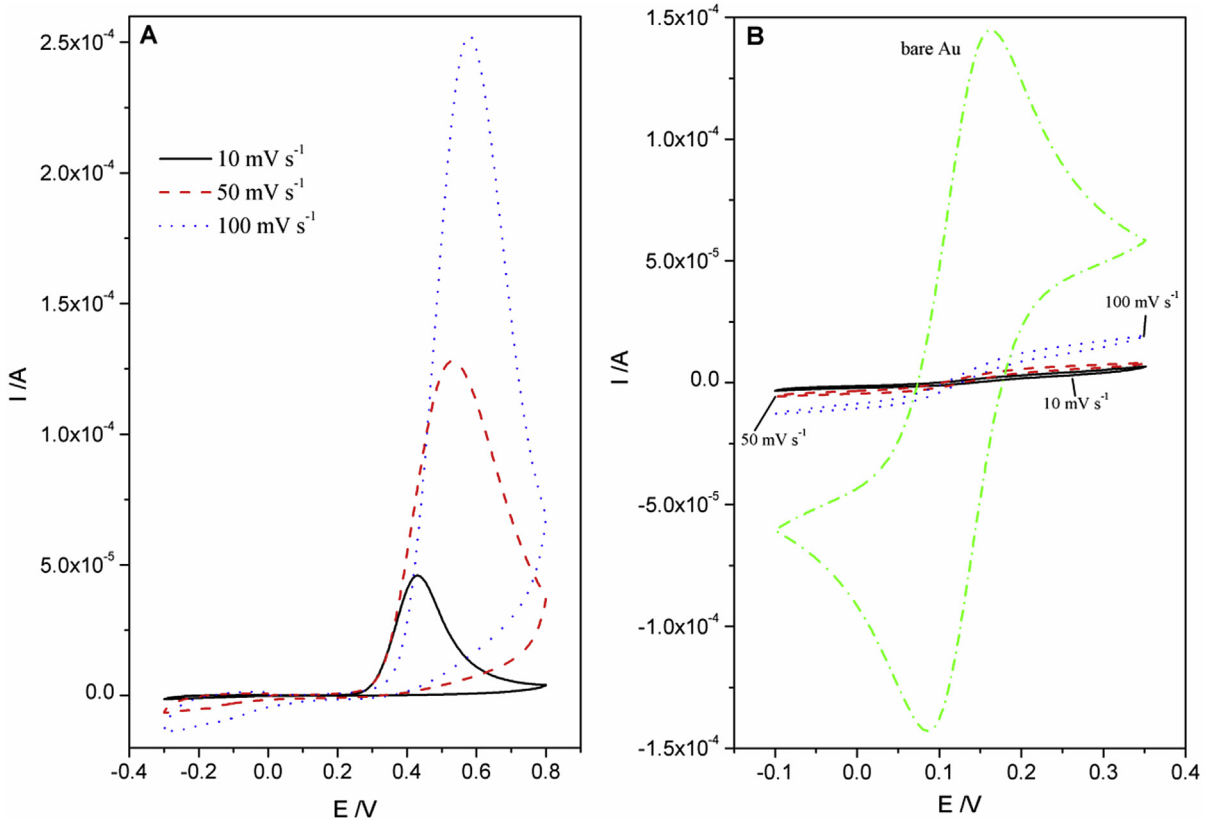

Fig. 1. (A) Cyclic voltammetric electropolymerization of 10 mM Ph in 0.1 M PBS pH 7.0 on AuSPEs using different scan rates: (—) 10 mV s^{-1}, (– –) 50 mV s^{-1} and (…) 100 mV s^{-1}. Number of scans: 1. (B) CVs recorded in the presence of 5 mM $[Fe(CN)_6]^{3-/4-}$ redox probe after the electrodeposition of Ph on AuSPEs at the different scan rate tested. For comparison, the voltammogram obtained with bare gold electrode was included in the figure. Scan rate: 50 mV s^{-1}.

the electrode surface confirmed by the disappearance of the redox peaks of ferro/ferricyanide probe when comparing to the voltammogram obtained at bare AuSPE. However, a close look of data obtained indicate that electropolymerization of polyphenol at 100 mV s^{-1} led to less insulating surface, which can be an advantage for the successful extraction of the protein from the MIP film. Thus, a scan rate of 100 mV s^{-1} during electropolymerization of Ph was used for the preparation of MIP receptor surface.

After the selection of scan rate, the film thickness was further adjusted by the study of the number of voltammetric cycles (1, 2, 5 and 10 cycles) performed during Ph electropolymerization used for preparation of MIP receptor surfaces. As an example, the voltammograms recorded during electrodeposition of Ph using 10 cycles electropolymerization are shown in Fig. 2A. The CV depicts a decreasing current during the oxidation process (~0.7 V) from the 1st cycle to the 10th cycle, indicating the deposition of the non-conducting polymer film on the AuSPE.

After extraction of Myo from MIP film with 20 mM SDS in 0.1 M PBS pH 7.0/methanol (10:1, v/v) solution overnight, the surfaces prepared with increasing number of voltammetric cycles were characterized with voltammetric measurements in the presence of ferro/ferricyanide probe, as shown in Fig. 2B. As can be seen, a significant decrease in redox peak current of ferro/ferricyanide probe was observed with the increasing number of cycles during the electropolymerization. Furthermore, Myo is highly retained in the polymer matrix after 5 or more electropolymerization cycles. Thus, the formation of ultrathin polymer films on the transducer surface was preferred to improve the sensitivity of the devices and 1 cycle electropolymerization was adopted in the construction of Myo MIP receptor film.

The thickness of the resulting polyphenol film was estimated by coulometric analysis after electropolymerization of Ph onto a bare AuSPE (NIP electrode, Fig. 1A, v = 100 mV s^{-1}). The following equation was used [22,38]:

$$d = \frac{MQ}{FA\rho} \quad (1)$$

where d is the thickness of the film, M is the molecular weight of the Ph monomer (94.11 g mol^{-1}), Q is the total charge transferred during the electropolymerization (obtained by integration of the voltammogram; see Fig. S2), F is the Faraday constant (9.6485 × 10^4 C mol^{-1}), A is the surface area of the electrode (0.126 cm^2), and ρ is the density of the polymer. Under the electropolymerization conditions described above, Q is about 5.64 × 10^{-5} C, and assuming that the density of polyphenol is similar to that of Ph ($\rho \approx 1$ g cm^{-3}), the thickness of the resulted film is about 4.4 nm.

According to Cai et al. [27], electronic nanosensors capable of recognizing proteins continue to be a challenge to implement in part because the MIP film may attenuate signals generated in response to template binding due to the large thickness. In this work, the thickness of the polyphenol nanocoating was found to be comparable to the protein diameter (single Myo molecule dimensions are about 4.5 nm × 3.5 nm × 2.5 nm [39]), so the electrochemical response of the MIP receptor to template protein binding is expected to be significantly enhanced after the optimization of the MIP film thickness.

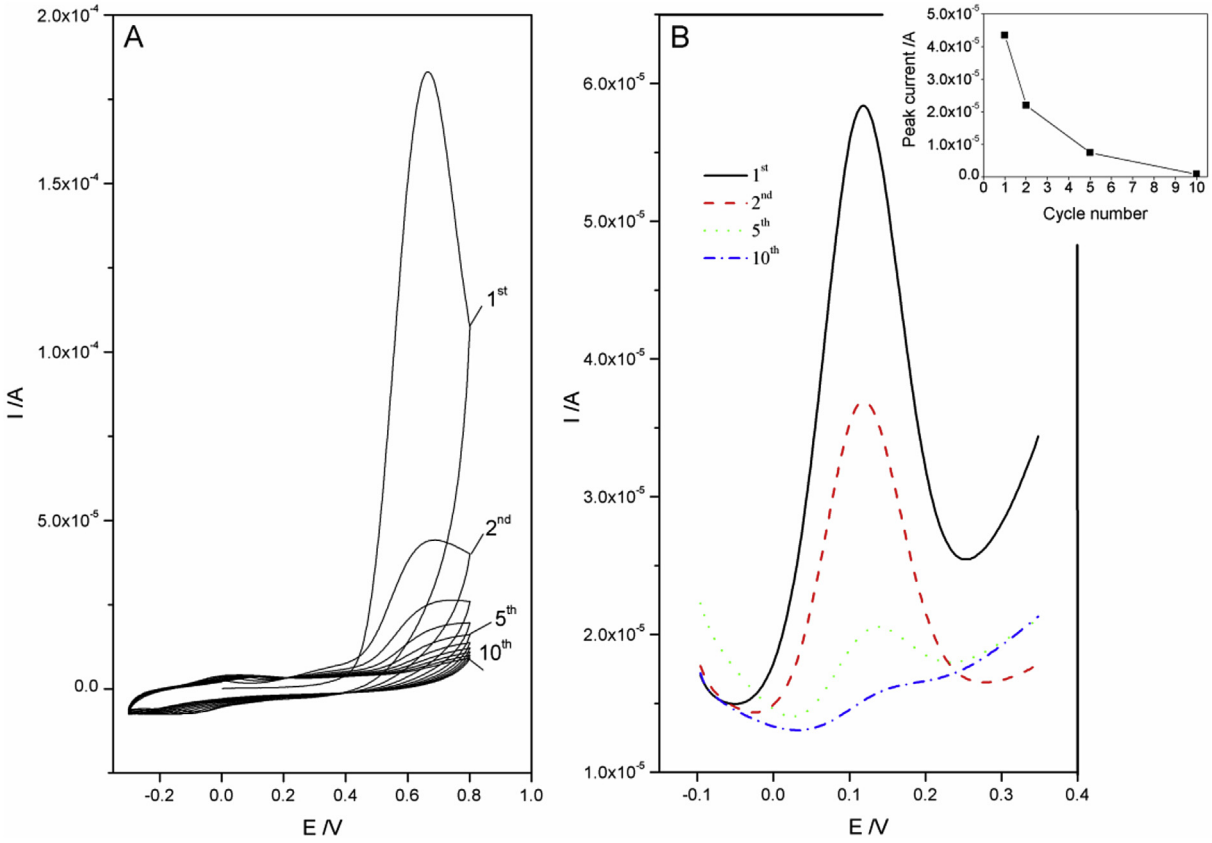

Fig. 2. A) Cyclic voltammetric deposition of 10 mM Ph in the presence of 5 mg mL^{-1} Myo in 0.1 M PBS pH 7.0. Scan rate: 100 mV s^{-1}; Number of scans: 10. B) SWVs recorded in the presence of 5 mM $[Fe(CN)_6]^{3-/4-}$ redox probe after extraction of the template protein from MIP surface with 20 mM SDS in 0.1 M PBS pH 7.0/methanol solution (10:1) overnight using 1, 2 5 and 10 cycles during electropolymerization of Ph. Inset: Peak currents obtained after protein extraction as a function of the number of cycles during electropolymerization of Ph.

3.2. Optimization of template concentration

The formation of specific imprints in polymers in based upon template-functional monomer interactions that cause the complexation of the artificial binding site (see Scheme 1). Thus, optimization of MIP formulation components requires the achievement of an optimum ratio of functional monomer/template.

MIP receptor film was prepared with increasing amounts of Myo (from 10 μg mL^{-1} to 5 mg mL^{-1}) while keeping the monomer concentration constant (C = 10 mM). EIS measurements collected before and after washing the MIP surfaces with 20 mM SDS in 0.1 M PBS pH 7.0 overnight are shown in Fig. 3. For comparison, NIP surfaces prepared in absence of template molecule was also included as Fig. 3D.

The electropolymerization of Ph in the presence of 5 mg mL^{-1} of template molecule resulted in formation of a high insulating medium (i.e., high R_{ct}) at the AuSPE surface (Fig. 3A, curve 1), while, after template extraction from the MIP modified surface, a large decrease of R_{ct} was observed (Fig. 3A, curve 2). A moderate incorporation of Myo in polyphenol film was observed when using 0.5 mg mL^{-1} of template molecule (Fig. 3B, curve 1), however, after washing out template protein the R_{ct} remains at very high values (Fig. 3B, curve 2) revealing a deficient MIP formation since template protein is very embedded within the polymeric matrix due to the reduced number of molecules in polymerization solution and therefore the extraction is difficult. Finally, the use of 10 μg mL^{-1} of template was not suitable for MIP receptor preparation since almost no protein was retained within the polymeric matrix (Fig. 3C, curve 1). The electrochemical impedance profile obtained under this condition is very similar to the one obtained at the NIP surface (Fig. 3D, curves 1 and 2).

Thus, the use of 5.0 mg mL^{-1} template concentration resulted in the increase of the number of binding sites formed at the MIP surface and enhanced the performance of the sensor [40,41].

3.3. Protein imprinting

Fabrication of the MIP film was achieved by cyclic voltammetric electrodeposition of 10 mM Ph in 0.1 M PBS pH 7.0 on AuSPE in the presence of 5 mg mL^{-1} Myo. The isoelectric point of Myo is 7.0 [32], so in the medium used the protein is its zwitterionic form. In aqueous environment, the protein will interact with Ph monomers due to non-covalent π interactions and H-bonds between the electron rich phenyl ring and the hydroxyl substituent of Ph and the N-H/C-H/positively charged residual groups of Myo [16,42–44]. The template-monomer complexes formed in solution are preserved till electropolymerization of Ph occurs and protein molecules are physically entrapped within the polymer matrix produced at the electrode surface.

Data recorded during the electropolymerization process shows the inhibition of Ph oxidation in the presence of Myo (Fig. 2A, 1st cycle) when compared with the electropolymerization in absence of template molecule (Fig. 1A, v = 100 mV s^{-1}) which was attributed to the additional barrier caused by the entrapment within the polymeric matrix (and due to some adsorption at the Au surface) of the non-conductive protein. Furthermore, voltammetric measurements in the presence of ferro/ferricyanide redox probe performed in the MIP receptor surface (Fig. 4A, curve 1) confirmed a smaller

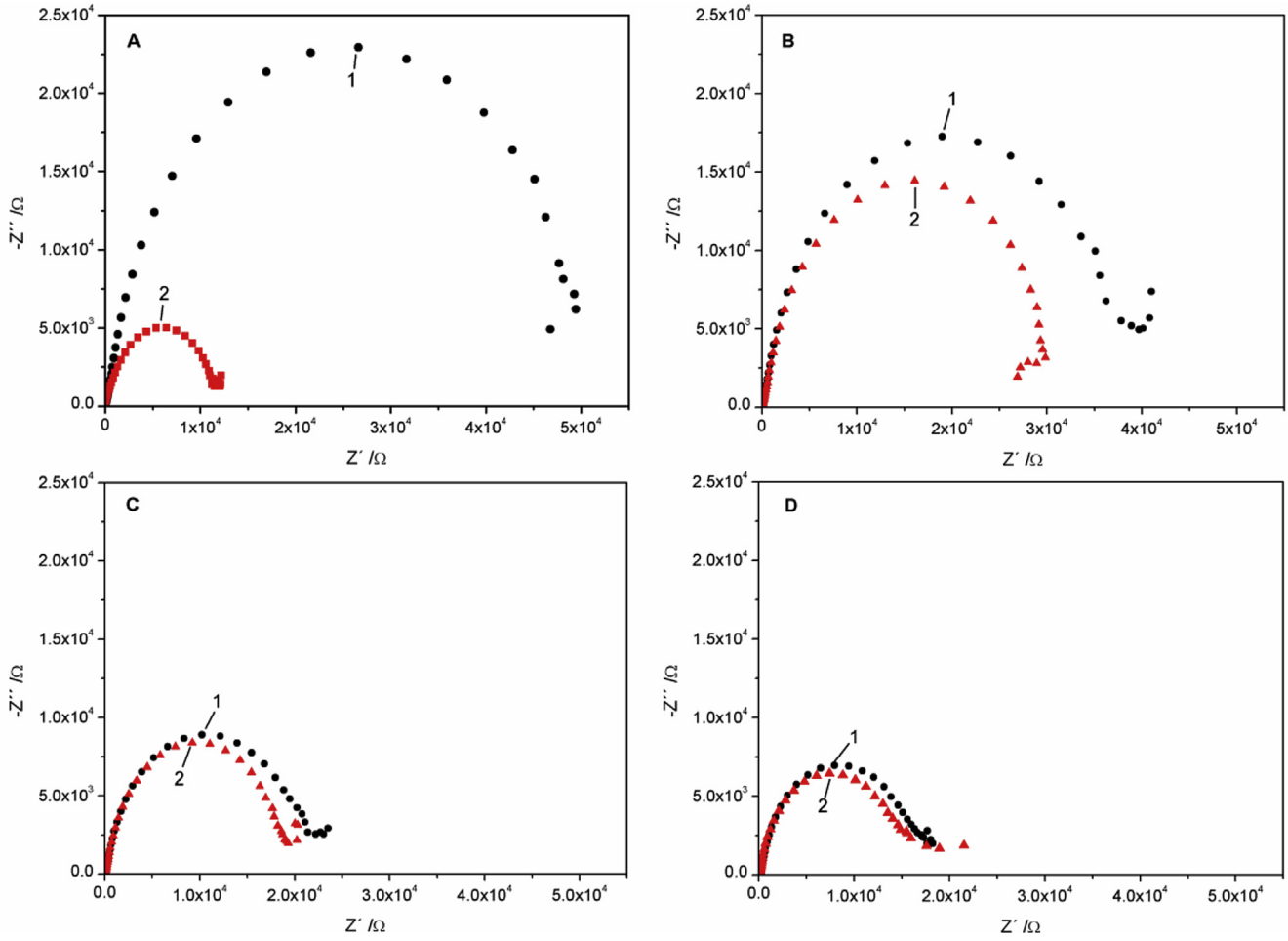

Fig. 3. Complex impedance plots obtained in presence of 5 mM $[Fe(CN)_6]^{3-/4-}$ redox probe before (curves 1) and after (curves 2) extraction of template protein with 20 mM SDS in 0.1 M PBS pH 7.0/methanol solution (1:10) for MIP surfaces prepared by electropolymerization of 10 mM Ph in 0.1 M PBS pH 7.0, at 100 mV s^{-1}, with 1 scan, using different template concentrations: A) 5 mg mL^{-1}, B) 0.5 mg mL^{-1} and C) 10 μg mL^{-1}. D) For compassion, data obtained at NIP surface in the absence of Myo was also included in the figure.

voltammetric peak than the voltammetric peak obtained at the NIP surface (Fig. 4B, curve 1) used as reference system due to the incorporation of Myo within the polymer layer in MIP system.

3.4. Extraction of template protein

The washing conditions used for template removal from formed polymer matrix need to be carefully selected and optimized in order to preserve the integrity of the imprinted sites, while removing as much template as possible [45], otherwise the application of the protein MIP receptor in quantitative analysis can be compromised.

In this work, several solvents (or solvent mixtures), containing or not additives were investigated aiming the selection of a suitable medium to perform the dissolution and/or denaturation necessary to the release of the template protein from the MIP polymer layer.

Some of the treatment conditions explored were based on mildly acidic or basic solutions (namely, 0.01–1 M H_2SO_4 during from 10 min to 2 h, 0.1 M H_2SO_4/ethanol (1:2, v/v) for 2 h, 1 M oxalic acid for 2 h, 1 M NaOH for 2 h and 0.25 M NaOH/ethanol (1:2, v/v) for 2 h) and on pure or mixed organic solvents (such as methanol, dimethyl sulfoxide, acetonitrile and water/ethanol mixture (1:2, v/v) for 2 h). Although some of the washing procedures appear to remove the protein from MIP films, degradation of the polyphenol was observed on NIP electrodes when acidic/basic conditions where used. Furthermore, after exposing the MIP surfaces to organic solvents no signs of quantitative protein removing was observed while experiments performed with NIP electrodes reveal some undesired reactions between the organic solvents used and polyphenol.

An enzymatic protein digestion approach was also tested to remove Myo from imprinted polymers. After incubation of the MIP films with trypsin (0.5–1 mg mL^{-1}, prepared in PBS 0.1 M pH 7.8) from 24 to 48 h in the dark, partial release of Myo from the polymer was observed (see Fig. S3). However, according to literature consulted, using enzymes for protein extraction run the risk of leaving template fragments attached to the polymer [46,47]. In addition, a considerable undesired adsorption of trypsin on NIP surface has occurred and the digestion procedure was not considered to be suitable for protein extraction.

Among the extraction procedures employed, the immersion of the modified electrodes in a 0.1 M PBS pH 7.0/methanol (10:1, v/v) solution containing 20 mM SDS overnight, followed by subsequent washing with pure water, was found to be the most effective process to remove Myo from the MIP polymeric matrix. The voltammetric measurements performed in the presence of ferro/ferricyanide redox probe performed at MIP surfaced shows a significant increase of the peak current after the template removal from the imprinted surfaces with the solution containing the surfactant (Fig. 4A, curve 2) while the voltammograms obtained at the analogous NIP surface, shown in Fig. 4B, revealed only a slight

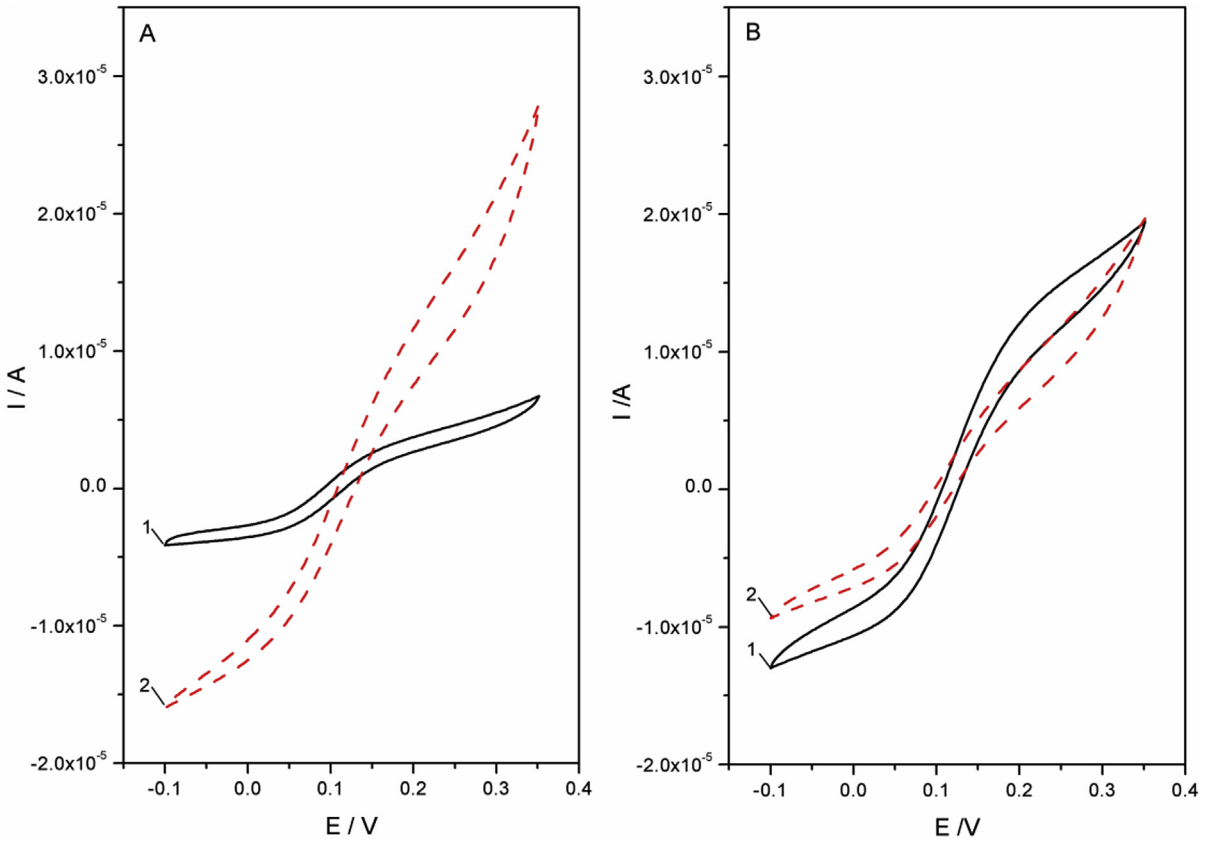

Fig. 4. CVs obtained in presence of 5 mM $[Fe(CN)_6]^{3-/4-}$ redox probe with MIP (A) and NIP (B) modified AuSPEs before (curves 1) and after (curves 2) extraction of template protein with 20 mM SDS in 0.1 M PBS pH 7.0/methanol (10:1, v/v) solution overnight.

decrease of voltammetric peak current of the redox probe after surface treatment with the extraction solution. Data obtained by EIS (see Fig. 3) also supported the physical entrapment of Myo within the electrogenerated non-conducting polymeric matrix followed by effective template wash out from MIP surface. The R_{ct} decreased from 51 kΩ to 11 kΩ (i.e. decrease of 78%) after extraction of Myo from the MIP surface (Fig. 3A) while R_{ct} values remained very low (around 16 kΩ) before and after exposing the NIP surface to the extraction solution (Fig. 3D) confirming that no severe damage in the polymer network was induced by the selected washing procedure.

Raman measurements were performed to confirm to the modification of the Au surfaces with the synthetic receptor polymeric film. Raman spectra recorded in the frequency range between 200 and 1900 cm^{-1} for MIP and NIP films are shown in Fig. 5A and Fig. 5B, respectively. The spectra of the AuSPE before any surface modification acted as reference spectra and showed one Raman band at 544 cm^{-1} that was attributed to the well-documented Au-O stretching vibration [48].

The modification of the electrode surface with the MIP film gave rise to a wide range of Raman absorption bands due to the presence of Myo inside of the polymer film. Some of the characteristic bands of Myo were identified in the MIP film spectra, namely [49,50]: bands at 1638 cm^{-1} ($\nu(C_\alpha C_m)_{asym}$, strong), 1585 cm^{-1} ($\nu(C_\alpha C_m)_{asym}$, strong), 1371 (Fe^{3+})/1342 (Fe^{2+}) cm^{-1} (ν(pyr half-ring)$_{sym}$, medium), 1310 cm^{-1} ($\nu(C_\alpha C_\beta)$, medium), 1171 cm^{-1} (ν(pyr half-ring)$_{sym}$, weak), 1130 cm^{-1} ($\nu(C_\alpha N)$, weak) and 750 cm^{-1} (ν(pyr breathing); $\nu(C_\alpha C_\beta)$, very weak). On the other hand, band intensities decreased dramatically for the non-imprinted polyphenol film and only a spectral band at around ~1600 cm^{-1} (ν(C=C) in benzene ring [51,52]) was observed. The presence of other bands in the Ph monomer spectra that did not appear in the NIP film spectra which can be explained by the extremely thin film of polyphenol covering the electrode surface whose Raman signal is almost indistinguishable from the bare Au signal. A decrease of the bare Au band intensity was also observed after modification of the electrode surface with the NIP film, confirming the successful modification of the AuSPE.

Raman measurements were also performed after protein extraction from the MIP film and the spectra recorded is shown in Fig. 5C. As expected, the Raman spectra of MIP and NIP materials are very similar confirming that the effective template removal from the MIP film and the resulting polymeric network has roughly the same chemical composition as the NIP film.

3.5. Analytical performance of the MIP sensor

In order to investigate the binding performance of the Myo imprinted polymer, the target protein was incubated on the MIP surface for 10 min with the binding buffer (0.1 M PBS pH 7.0) containing increasing concentrations of Myo, followed by washing. SWV were used to monitor the ferro/ferricyanide probe response upon Myo binding on the MIP receptor surface because it provided a better peak resolution comparing to CV and it is usually more sensitive to smaller changes in the concentrations of target analyte.

Fig. 6A represents the decrease of redox peak currents of the ferro/ferricyanide couple for an increase in Myo concentration from 0.001 ng mL^{-1} to 100 μg mL^{-1}. Successful rebinding of the template protein was observed. The investigation of the binding performance was made also using NIP electrodes (Fig. 6B). The polymer film deposited on the electrode in the absence of Myo, but treated the same way as that of MIP, did not show a decrease of redox peak

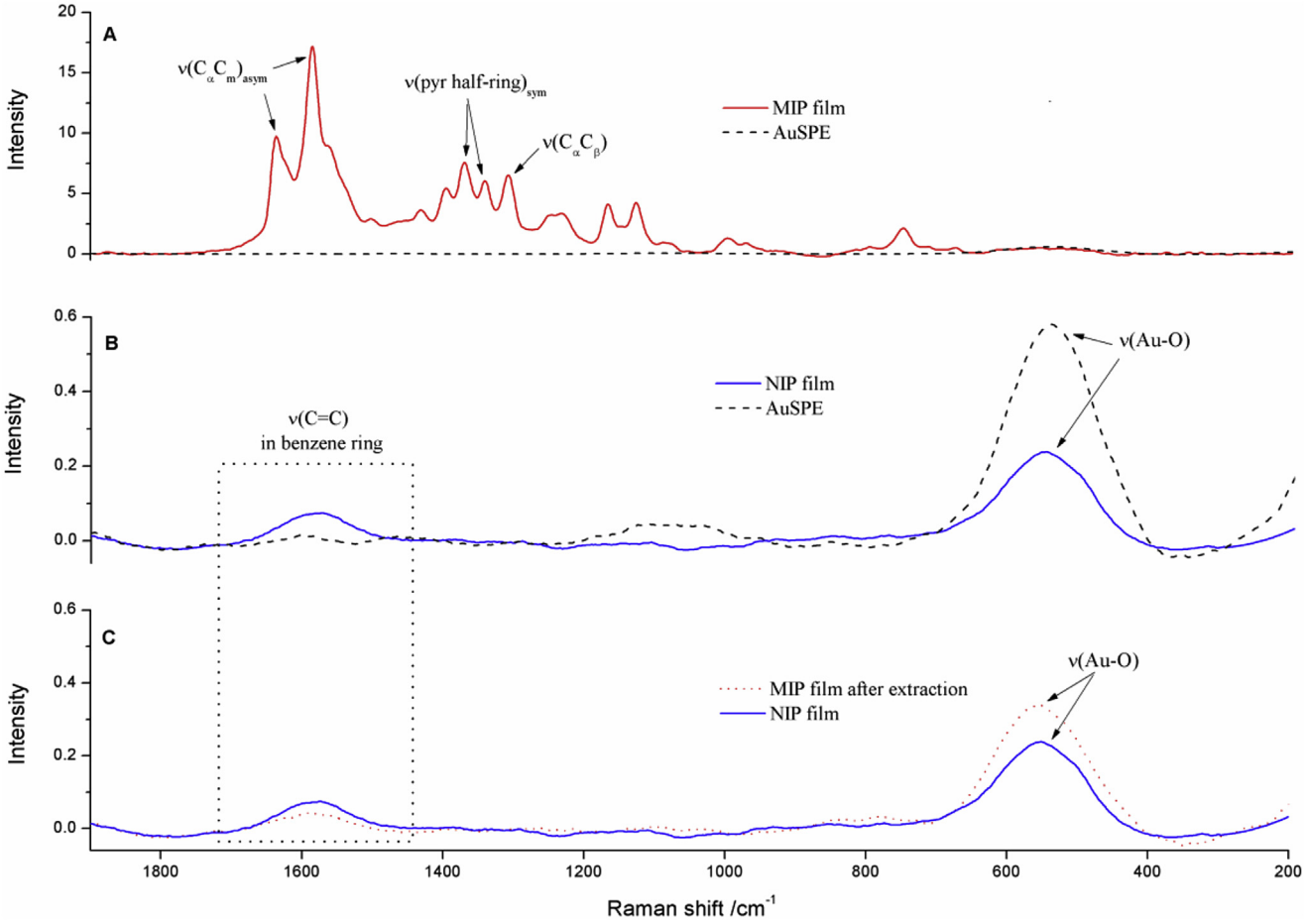

Fig. 5. Raman spectra obtained for AuSPE modified with A) MIP film, B) NIP film and C) MIP film after template extraction. For comparison, the spectra of bare AuSPE was also included in the figure. Savitzky-Golay filter was used for smoothing and differentiation of the collected spectra.

current with the increasing concentration of Myo.

In Fig. 6C, the peak current obtained by SWV was plotted as a function of the logarithm of Myo concentration (in ng mL^{-1}). Good linearity was achieved ($R^2 = 0.993$) over the concentration range used. In the NIP sensor (inset of Fig. 6C), the peak current showed an apparent random (non-linear) behaviour with the increasing concentration of Myo. As expected, the presence of Myo did not affect the response of the NIP electrode. This evidence suggested that the recognition of Myo on the MIP surface was made through the imprinted sites and the contribution of non-specific response was negligible or absent.

The LOD obtained by the MIP sensor was calculated according to Recommendations of IUPAC for ion-selective electrodes [53]. The calculated LOD was 2.1 pg mL^{-1}, using the SWV technique. The LOD obtained was significantly lower than other LODs reported in literature (of few μg mL^{-1}) for Myo detection using MIP biosensor technology based on acrylamide [28–30] and *o*-aminophenol [31] polymers, allowing the detection of the protein biomarker below the threshold needed to detect myocardial infarction (cut-off levels between 70 and 200 ng mL^{-1} [1]).

From this data it was possible to estimate the binding affinity in the MIP system by adjusting the experimental data to the Freundlich isotherm:

$$\frac{I_0 - I}{I_0} = K_F \cdot C_e^{1/n_F} \quad (2)$$

where K_F is the Freundlich constant, n_F the Freundlich exponent, $(I_0\text{-}I)/I_0$ is the adsorbed amount at equilibrium and C_e (ng mL^{-1}) the equilibrium concentration. The fit of the binding isotherm of Myo to the MIP and NIP synthetic receptor films is shown in Fig. 6D. An impressive ~8 fold increase in the binding affinity of Myo to MIP ($K_F = 0.119 \pm 0.002$ ng^{-1} mL) as compared to the NIP ($K_F = 0.015 \pm 0.002$ ng^{-1} mL) was obtained. The significant difference in the interaction between template and binding sites present in the two polymer matrices (MIP and NIP films) demonstrated the effectiveness of this approach in creating a high affinity synthetic receptor for the target protein.

High values of n_F were obtained for MIP ($n_F = 23 \pm 1$) and NIP ($n_F = 25 \pm 13$) systems. This meant that for low concentration levels the amount of bound protein increased greatly with small changes in C_e, while at larger concentrations of protein more imprinted sites were rebound and the adsorption intensity weakened and approached a constant value (saturation occurred and the analytical signal remained constant).

3.6. Analytical application feasibility

In order to investigate the usability of the developed MIP sensor in the presence of interfering components, diluted artificial serum (1:10, in 0.1 M PBS pH 7.0) was used. SWV was employed to monitor the ferro/ferricyanide probe redox signal upon binding of Myo at the modified surface. The voltammograms collected for the different Myo concentrations prepared in diluted artificial serum

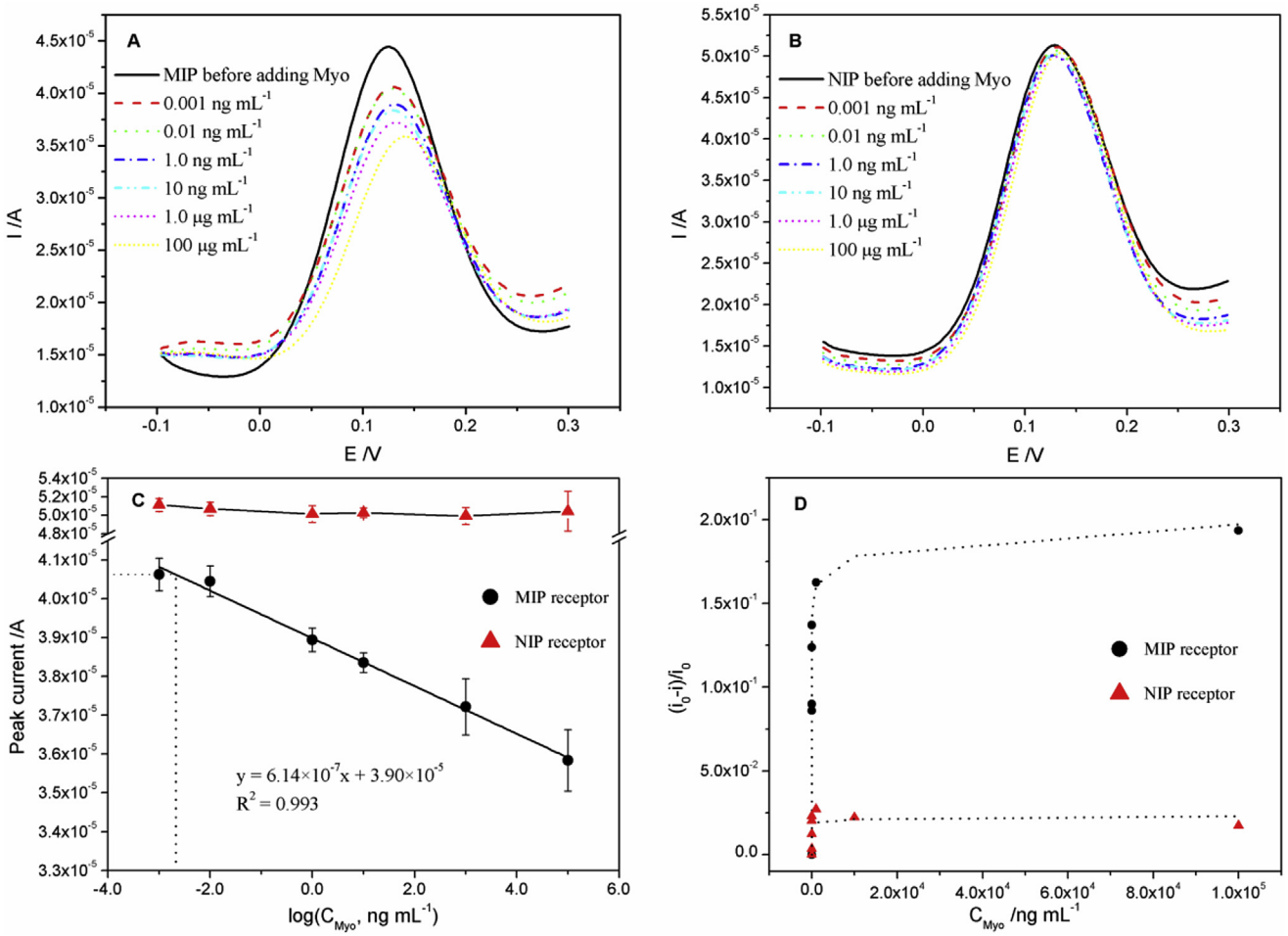

Fig. 6. Electrochemical evaluation in presence of 5 mM $[Fe(CN)_6]^{3-/4-}$ redox probe of template rebinding with (A) MIP and (B) NIP receptor films, after incubation in different concentrations of Myo (from 0.001 ng mL^{-1} to 100 µg mL^{-1}, in 0.1 M PBS pH 7.0) for 10 min. C) The plots of peak current *versus* Myo concentration on MIP and NIP receptor films. Dotted lines represents LOD estimation. D) Binding isotherm of synthetic MIP and NIP receptor films at different concentrations of Myo. Dotted lines represents the fitting of Freundlich isotherm to the experimental data.

were used and the correlation between the peak current and the concentration of Myo identified. The corresponding data/plots are shown in Fig. 7.

The sensitivity of the Myo MIP biosensor in the diluted artificial serum (-6.69×10^{-7} A/decade C_{Myo}, ng mL^{-1}) was of the same order of magnitude of that obtained in BPS (-6.14×10^{-7} A/decade C_{Myo}, ng mL^{-1}) allowing to conclude that of the serum matrix had no apparent significant contribution to the analytical signal. It also suggested that the observed decrease of redox probe response was only due to the specific binding of Myo in diluted serum to the MIP receptor film. The LOD was 14 pg mL^{-1}. The increase of the LOD obtained from 2.3 pg mL^{-1} in PBS to 13 pg mL^{-1} in serum was attributed to the reduction of the linear concentration range in diluted serum (from 0.01 ng mL^{-1} to 100 µg mL^{-1}), when compared to the linear concentration range obtained in PBS (from 0.001 ng mL^{-1} to 100 µg mL^{-1}). However, the MIP sensor prepared was still able to detect Myo in serum samples at clinically relevant concentration levels.

Recovery studies performed with MIP sensor were conducted in diluted serum samples spiked with known amounts of Myo. The concentration values, calculated from the standard calibration curve after duplicate measurements performed on the samples tested, are shown Table 1.

Recovery is a very important indication of the accuracy of the MIP sensor for Myo detection in serum samples. Although the error affecting the concentration found ranges from 2% to 28%, these error levels were considered to be acceptable due to the large concentration range of the MIP biosensor when compared to the slow variation of the electroanalytical response.

4. Conclusion

The molecular imprinting approach was adopted in this work for the simple design of a synthetic protein receptor biosensor with the intention of mimic the biological antibody model for the detection of cardiac biomarker myoglobin with high affinity and specificity. The miniaturized point-of-care MIP biosensor was prepared by electropolymerization of phenol, conducted by cyclic voltammetry, on a AuSPE, in the presence of the target protein.

The fabrication of an extremely thin MIP polymer of ~4.4 nm (approximately the same size of template protein) was considered of great importance in order to increase the analytical response and the performance of the electrochemical sensor towards the protein.

The synthetic receptor for Myo was evaluated by observing the effect of protein binding on the electrochemistry of a well-characterized redox probe. It showed the successful extraction of the protein from the polymer, after treating the MIP surface with the washing procedure adopted, a solution mixture containing SDS. (Re)binding affinity studies, performed by fitting Freundlich isotherm to experimental data, indicated excellent affinity of the

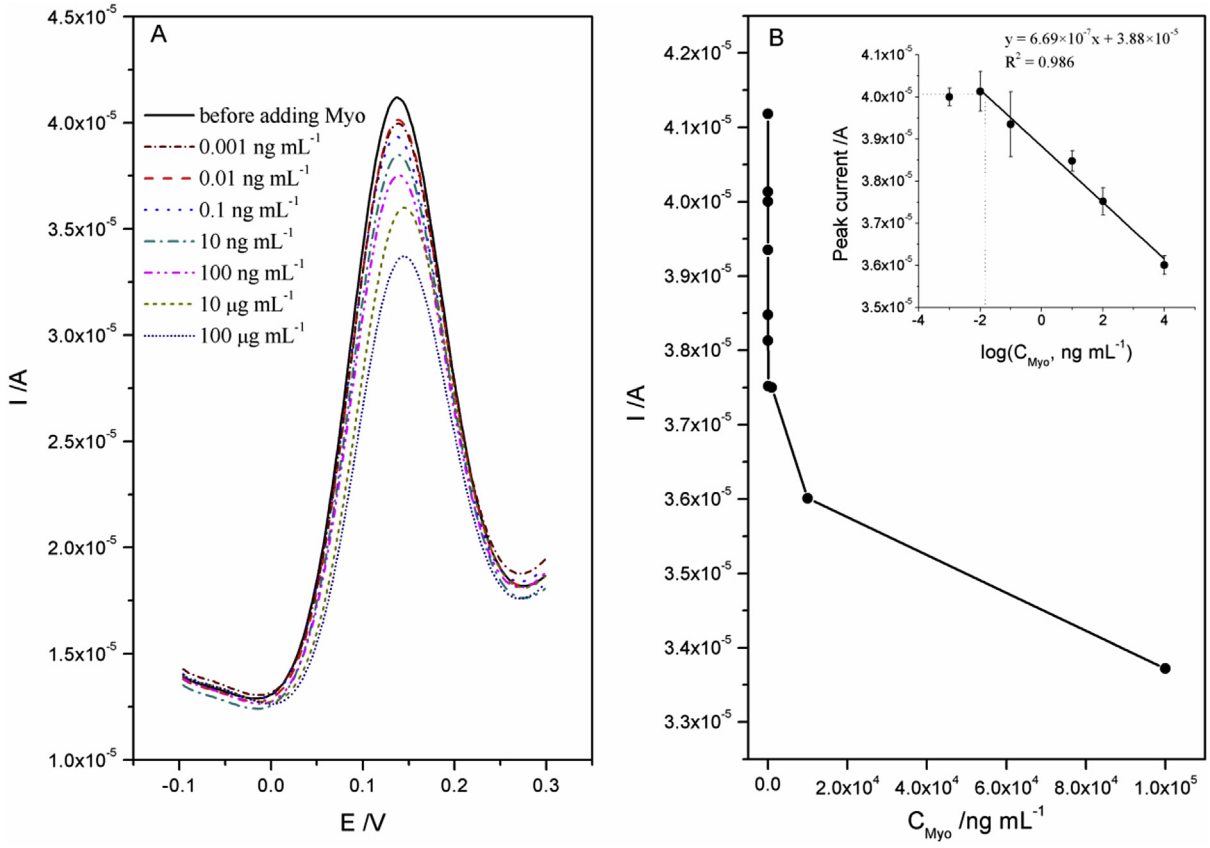

Fig. 7. A) SWVs obtained in presence of 5 mM $[Fe(CN)_6]^{3-/4-}$ redox probe with MIP receptor film after incubation in different concentrations of Myo (from 0.001 ng mL^{-1} to 10 µg mL^{-1}, in diluted artificial serum) for 10 min. B) Relationship between the peak current and the concentration of Myo in diluted artificial serum. Inset: The plot of peak current *versus* Myo concentration in logarithmic coordinates. Dotted lines represents LOD estimation.

Table 1
Recovery studies performed with MIP sensor for diluted artificial serum samples spiked with Myo at different concentration.

Sample	Added /ng mL^{-1}	Found /ng mL^{-1}	% Recovery
1	0.60	0.5 ± 0.4	128
2	500	490 ± 59	98

MIP synthetic receptor film for the imprinted protein (~8 fold when compared to NIP, based on obtained K_F values).

The selective adsorption of Myo onto MIP film (after 10 min incubation) induced a significant reduction of the redox probe currents. Calibration plots obtained showed a linear dependency of peak current over an extremely wide Myo concentration range (from few ng mL^{-1} to several µg mL^{-1}). LODs obtained (of 2.1 pg mL^{-1} in buffer and 14 pg mL^{-1} in artificial serum) showed that the MIP sensor was capable of detecting Myo at clinically relevant levels (cut-off values).

Most notably, the LODs obtained by the fabricated MIP sensors are of the same order of magnitude of those obtained by natural receptors methodologies, showing that the prepared Myo synthetic receptor film possesses remarkable recognition properties. Moreover, the inherent characteristics of a rigid polymer may lead to greater robustness, long long-term storage stability and potential re-usability of the MIP biosensor when compared to biosensors based on natural receptors, while remaining inexpensive.

Acknowledgments

This research was carried out with financial support of FCT (Fundação para a Ciência e Tecnologia) through the strategic Project PEst-C/QUI/UI0081/2014) awarded to CIQUP and NORTE-2020 through the project NORTE-01-0145-FEDER-000029 (application NORTE-45-2015–02). José Ribeiro (ref. SFRH/BPD/105395/2014) acknowledges FCT under the QREN – POPH – Advanced Training, subsidized by European Union and national MEC funds. José Ribeiro acknowledges Ana Patrícia Tavares Moreira for the support provided during Raman measurements.

Appendix A. Supplementary data

Supplementary data related to this article can be found at http://dx.doi.org/10.1016/j.aca.2017.05.017.

References

[1] A. Qureshi, Y. Gurbuz, J.H. Niazi, Biosensors for cardiac biomarkers detection: a review, Sensors Actuators B Chem. 171–172 (2012) 62–76.
[2] B. McDonnell, S. Hearty, P. Leonard, R. O'Kennedy, Cardiac biomarkers and the case for point-of-care testing, Clin. Biochem. 42 (7–8) (2009) 549–561.
[3] Z. Yang, D. Min Zhou, Cardiac markers and their point-of-care testing for diagnosis of acute myocardial infarction, Clin. Biochem. 39 (8) (2006) 771–780.
[4] J.C. Kendrew, R.G. Parrish, J.R. Marrack, E.S. Orlans, The species specificity of myoglobin, Nature 174 (4438) (1954) 946–949.
[5] B.A. Wittenberg, J.B. Wittenberg, Transport of oxygen in muscle, Annu. Rev. Physiol. 51 (1) (1989) 857–878.
[6] M. Wolf, D. Juncker, B. Michel, P. Hunziker, E. Delamarche, Simultaneous detection of C-reactive protein and other cardiac markers in human plasma using micromosaic immunoassays and self-regulating microfluidic networks, Biosens. Bioelectron. 19 (10) (2004) 1193–1202.
[7] J. Masson, T.M. Battaglia, P. Khairallah, S. Beaudoin, K.S. Booksh, Quantitative measurement of cardiac markers in undiluted serum, Anal. Chem. 79 (2)

(2007) 612–619.
[8] L. Tang, K.A. Kang, Preliminary study of fiber optic multi-cardiac-marker biosensing system for rapid coronary heart disease diagnosis and prognosis, in: G. Cicco, D.F. Bruley, M. Ferrari, D.K. Harrison (Eds.), Oxygen Transport to Tissue XXVII, Springer US, Boston, MA, 2006, pp. 101–106.
[9] W. Wu, Z. Bian, W. Wang, J. Zhu, PDMS gold nanoparticle composite film-based silver enhanced colorimetric detection of cardiac troponin I, Sensors Actuators B Chem. 147 (1) (2010) 298–303.
[10] I. Cho, E. Paek, Y. Kim, J. Kim, S. Paek, Chemiluminometric enzyme-linked immunosorbent assays (ELISA)-on-a-chip biosensor based on cross-flow chromatography, Anal. Chim. Acta 632 (2) (2009) 247–255.
[11] V.V. Shumyantseva, T.V. Bulko, M.Y. Vagin, E.V. Suprun, A.I. Archakov, Electrochemical immunoanalysis of cardiac myoglobin, Biochemistry (Moscow), Suppl. Ser. B Biomed. Chem. 4 (3) (2010) 237–242.
[12] E.V. Suprun, A.L. Shilovskaya, A.V. Lisitsa, T.V. Bulko, V.V. Shumyantseva, A.I. Archakov, Electrochemical immunosensor based on metal nanoparticles for cardiac myoglobin detection in human blood plasma, Electroanalysis 23 (5) (2011) 1051–1057.
[13] A. Qureshi, Y. Gurbuz, J.H. Niazi, Label-free detection of cardiac biomarker using aptamer based capacitive biosensor, Procedia Eng. 5 (2010) 828–830.
[14] M.J. Whitcombe, I. Chianella, L. Larcombe, S.A. Piletsky, J. Noble, R. Porter, A. Horgan, The rational development of molecularly imprinted polymer-based sensors for protein detection, Chem. Soc. Rev. 40 (3) (2011) 1547–1571.
[15] C. Malitesta, E. Mazzotta, R.A. Picca, A. Poma, I. Chianella, S.A. Piletsky, MIP sensors – the electrochemical approach, Anal. Bioanal. Chem. 402 (5) (2012) 1827–1846.
[16] P.S. Sharma, A. Pietrzyk-Le, F. D'Souza, W. Kutner, Electrochemically synthesized polymers in molecular imprinting for chemical sensing, Anal. Bioanal. Chem. 402 (10) (2012) 3177–3204.
[17] Y. Liu, Y. Wang, Q. Dai, Y. Zhou, Magnetic deep eutectic solvents molecularly imprinted polymers for the selective recognition and separation of protein, Anal. Chim. Acta 936 (2016) 168–178.
[18] Y. Wang, M. Han, G. Liu, X. Hou, Y. Huang, K. Wu, C. Li, Molecularly imprinted electrochemical sensing interface based on in-situ-polymerization of amino-functionalized ionic liquid for specific recognition of bovine serum albumin, Biosens. Bioelectron. 74 (2015) 792–798.
[19] Y. Wang, M. Han, X. Ye, K. Wu, T. Wu, C. Li, Voltammetric myoglobin sensor based on a glassy carbon electrode modified with a composite film consisting of carbon nanotubes and a molecularly imprinted polymerized ionic liquid, Microchim. Acta 184 (1) (2017) 195–202.
[20] L. Ye, K. Mosbach, Molecular imprinting: synthetic materials as substitutes for biological antibodies and receptors, Chem. Mater. 20 (3) (2008) 859–868.
[21] P.N. Barlett, J.M. Cooper, A review of the immobilization of enzymes in electropolymerized films, J. Electroanal. Chem. 362 (1) (1993) 1–12.
[22] T.L. Panasyuk, V.M. Mirsky, S.A. Piletsky, O.S. Wolfbeis, Electropolymerized molecularly imprinted polymers as receptor layers in capacitive chemical sensors, Anal. Chem. 71 (20) (1999) 4609–4613.
[23] M.C. Blanco-López, S. Gutiérrez-Fernández, M.J. Lobo-Castañón, A.J. Miranda-Ordieres, P. Tuñón-Blanco, Electrochemical sensing with electrodes modified with molecularly imprinted polymer films, Anal. Bioanal. Chem. 378 (8) (2004) 1922–1928.
[24] Z. Wang, J. Kang, X. Liu, Y. Ma, Capacitive detection of theophylline based on electropolymerized molecularly imprinted polymer, Int. J. Polym. Analysis Charact. 12 (2) (2007) 131–142.
[25] M. Riskin, R. Tel-Vered, I. Willner, The imprint of electropolymerized polyphenol films on electrodes by donor-acceptor interactions: selective electrochemical sensing of N,N′-dimethyl-4,4′-bipyridinium (methyl viologen), Adv. Funct. Mater. 17 (18) (2007) 3858–3863.
[26] E. Granot, R. Tel-Vered, O. Lioubashevski, I. Willner, Stereoselective and enantioselective electrochemical sensing of monosaccharides using imprinted boronic acid-functionalized polyphenol films, Adv. Funct. Mater. 18 (3) (2008) 478–484.
[27] C. Dong, R. Lu, Z. Huaizhou, X. Chenjia, Z. Lu, Y. Ying, W. Hengzhi, L. Yucheng, M.F. Roberts, J.H. Chuang, M.J. Naughton, R. Zhifeng, T.C. Chiles, A molecular-imprint nanosensor for ultrasensitive detection of proteins, Nat. Nanotechnol. 5 (8) (2010) 597–601.
[28] F.T.C. Moreira, R.A.F. Dutra, J.P.C. Noronha, M.G.F. Sales, Electrochemical biosensor based on biomimetic material for myoglobin detection, Electrochimica Acta 107 (2013) 481–487.
[29] F.T.C. Moreira, R.A.F. Dutra, J.P.C. Noronha, J.C.S. Fernandes, M.G.F. Sales, Novel biosensing device for point-of-care applications with plastic antibodies grown on Au-screen printed electrodes, Sensors Actuators B Chem. 182 (2013) 733–740.
[30] F.T.C. Moreira, S. Sharma, R.A.F. Dutra, J.P.C. Noronha, A.E.G. Cass, M.G.F. Sales, Smart plastic antibody material (SPAM) tailored on disposable screen printed electrodes for protein recognition: application to myoglobin detection, Biosens. Bioelectron. 45 (2013) 237–244.
[31] F.T.C. Moreira, S. Sharma, R.A.F. Dutra, J.P.C. Noronha, A.E.G. Cass, M.G.F. Sales, Protein-responsive polymers for point-of-care detection of cardiac biomarker, Sensors Actuators B Chem. 196 (2014) 123–132.
[32] Y. Wang, Y. Zhou, J. Sokolov, B. Rigas, K. Levon, M. Rafailovich, A potentiometric protein sensor built with surface molecular imprinting method, Biosens. Bioelectron. 24 (1) (2008) 162–166.
[33] P.I. Iotov, S.V. Kalcheva, Mechanistic approach to the oxidation of phenol at a platinum/gold electrode in an acid medium, J. Electroanal. Chem. 442 (1–2) (1998) 19–26.
[34] N. Belhadj Tahar, A. Savall, Electrochemical removal of phenol in alkaline solution. Contribution of the anodic polymerization on different electrode materials, Electrochimica Acta 54 (21) (2009) 4809–4816.
[35] H.D. Graham, Stabilization of the Prussian blue color in the determination of polyphenols, J. Agric. Food Chem. 40 (5) (1992) 801–805.
[36] Ç. Sayıklı Şimşek, M. Nur Sonuç Karaboğa, M.K. Sezgintürk, A new immobilization procedure for development of an electrochemical immunosensor for parathyroid hormone detection based on gold electrodes modified with 6-mercaptohexanol and silane, Talanta 144 (2015) 210–218.
[37] J. Wang, M. Jiang, F. Lu, Electrochemical quartz crystal microbalance investigation of surface fouling due to phenol oxidation, J. Electroanal. Chem. 444 (1) (1998) 127–132.
[38] H. Liao, Z. Zhang, H. Li, L. Nie, S. Yao, Preparation of the molecularly imprinted polymers-based capacitive sensor specific for tegafur and its characterization by electrochemical impedance and piezoelectric quartz crystal microbalance, Electrochimica Acta 49 (24) (2004) 4101–4107.
[39] H. Lin, J. Rick, T. Chou, Optimizing the formulation of a myoglobin molecularly imprinted thin-film polymer—formed using a micro-contact imprinting method, Biosens. Bioelectron. 22 (12) (2007) 3293–3301.
[40] H.S. Andersson, J.G. Karlsson, S.A. Piletsky, A.-C. Koch-Schmidt, K. Mosbach, I.A. Nicholls, Study of the nature of recognition in molecularly imprinted polymers, II [1]: influence of monomer–template ratio and sample load on retention and selectivity, J. Chromatogr. A 848 (1–2) (1999) 39–49.
[41] H. Kim, D.A. Spivak, New insight into modeling non-covalently imprinted polymers, J. Am. Chem. Soc. 125 (37) (2003) 11269–11275.
[42] D.S. Janiak, P. Kofinas, Molecular imprinting of peptides and proteins in aqueous media, Anal. Bioanal. Chem. 389 (2) (2007) 399–404.
[43] A.C. Pierce, K.L. Sandretto, G.W. Bemis, Kinase inhibitors and the case for CH…O hydrogen bonds in protein–ligand binding, Proteins Struct. Funct. Bioinforma. 49 (4) (2002) 567–576.
[44] Y. Umezawa, M. Nishio, CH/π interactions in the crystal structure of class I MHC antigens and their complexes with peptides, Bioorg. Med. Chem. 6 (12) (1998) 2507–2515.
[45] N. Karimian, A.P.F. Turner, A. Tiwari, Electrochemical evaluation of troponin T imprinted polymer receptor, Biosens. Bioelectron. 59 (2014) 160–165.
[46] D.L. Venton, E. Gudipati, Influence of protein on polysiloxane polymer formation: evidence for induction of complementary protein-polymer interactions, Biochimica Biophysica Acta (BBA) - Protein Struct. Mol. Enzym. 1250 (2) (1995) 126–136.
[47] D.M. Hawkins, D. Stevenson, S.M. Reddy, Investigation of protein imprinting in hydrogel-based molecularly imprinted polymers (HydroMIPs), Anal. Chim. Acta 542 (1) (2005) 61–65.
[48] Y. Zhang, X. Gao, M.J. Weaver, Nature of surface bonding on voltammetrically oxidized noble metals in aqueous media as probed by real-time surface-enhanced Raman spectroscopy, J. Phys. Chem. 97 (33) (1993) 8656–8663.
[49] A. Rygula, K. Majzner, K.M. Marzec, A. Kaczor, M. Pilarczyk, M. Baranska, Raman spectroscopy of proteins: a review, J. Raman Spectrosc. 44 (8) (2013) 1061–1076.
[50] S. Hu, K.M. Smith, T.G. Spiro, Assignment of protoheme resonance raman spectrum by heme labeling in myoglobin, J. Am. Chem. Soc. 118 (50) (1996) 12638–12646.
[51] N. Oyama, T. Ohsaka, T. Hirokawa, T. Suzuki, Synthesis of conducting thin films by electro-oxidative polymerization of phenol, J. Chem. Soc. Chem. Commun. (15) (1987) 1133–1134.
[52] A. Shah, R. Holze, Poly(o-aminophenol) with two redox processes: a spectroelectrochemical study, J. Electroanal. Chem. 597 (2) (2006) 95–102.
[53] R.P. Buck, E. Lindner, Recommendations for nomenclature of ionselective electrodes (IUPAC Recommendations 1994), Pure Appl. Chem. (1994) 2527.